Science Advances
AAAS

advances.sciencemag.org/cgi/content/full/5/12/eaax7331/DC1

Supplementary Materials for

Sleep fragmentation, microglial aging, and cognitive impairment in adults with and without Alzheimer's dementia

Kirusanthy Kaneshwaran, Marta Olah, Shinya Tasaki, Lei Yu, Elizabeth M. Bradshaw, Julie A. Schneider, Aron S. Buchman, David A. Bennett, Philip L. De Jager, Andrew S. P. Lim*

*Corresponding author. Email: andrew.lim@utoronto.ca

Published 11 December 2019, *Sci. Adv.* **5**, eaax7331 (2019)
DOI: 10.1126/sciadv.aax7331

The PDF file includes:

Other Supplementary Material for this manuscript includes the following:

(available at advances.sciencemag.org/cgi/content/full/5/12/eaax7331/DC1)

Table S1 (Microsoft Excel format). Antemortem sleep fragmentation and expression of microglia and astrocyte marker genes: Gene level results.

Supplementary Materials and Methods

Assessment of Sleep Fragmentation and Circadian Disruption

Sleep fragmentation was assessed in the MAP cohort by actigraphy (Actical, Phillips Respironics, Bend, OR). Actigraphs were set to record in 15-sec epochs and placed on participants' non-dominant wrist by study staff, who returned 10 days later to remove them. Records were visually examined for periods of suspected device removal. In addition, any period 4 hours or greater with no activity counts at all was considered suspicious for device removal.

Sleep fragmentation, the extent to which sleep is interrupted by awakenings, was quantified in each recording with the metric k_{RA} as described and validated elsewhere (*14, 44*). The metric k_{RA} roughly represents the probability per 15-second period of having an arousal (as indicated by a non-zero activity count) following a period of sustained rest (>= ~5 minutes of inactivity). A greater degree of sleep fragmentation translates to a higher k_{RA}. k_{RA} correlates strongly with polysomnographic measures of sleep fragmentation (*14*).

Circadian disruption was quantified in each recording with the metric interdaily stability, a non-parametric measure of the day-to-day stability of activity patterns, as described elsewhere(*12*). Interdaily stability provides an indication of the extent to which a periodic time series is similar in shape from cycle to cycle. It ranges from 0 to 1; 0 indicates a complete lack of similarity from day to day, while 1 indicates perfect day-to-day similarity. We calculated interdaily stability from the first 7 days of each actigraphic record (containing 5 weekdays and 2 weekend days) using 1-hour bins and a 24-hour period.

In keeping with prior work with other risk factors (*37*), where more than one measurement was available for an actigraphic measure in a given individual, we took the average of all available measurements. This best reflects the cumulative impact of sleep fragmentation across the duration of the study, while minimizing the effects of individual measurements, which could be reflective of acute or terminal illness. Because many dementia-related pathologies accumulate over years, we believe the cumulative burden of sleep fragmentation over the course of the study is likely to have a greater influence on dementia-related pathologies than a single measurement proximate to death.

Assessment of Cognition

Participants underwent annual uniform structured cognitive evaluations consisting of a battery of 19 cognitive tests spanning 5 domains (episodic memory [logical Memory Ia, logical Memory IIa, immediate story recall, delayed story recall, word list memory, word list recall, word list recognition], semantic memory [Boston naming test, category fluency, national adult reading test], working memory [digit span forward, digit span backward, digit ordering], perceptual speed [symbol digit modalities test, number comparison, Stroop word reading, Stroop color naming], and visuospatial ability [judgment of line orientation, standard progressive matrices). As described previously (*45*), a composite measure for each domain was created by converting each test within each domain to a z-score and averaging the z-scores. The individual cognitive test z-scores were then averaged to create a composite global cognitive score scaled such that 0 represents the mean score of all participants at baseline, positive scores indicate better performance, and 1 unit represents approximately 1 standard deviation of performance. In addition to the above, participants were classified as having a clinical diagnosis of dementia by National Institute of Neurological And Communicative Disorders and Stroke-Alzheimer's Disease and Related Disorders Association criteria (*46*). Our primary cognitive outcome was composite global cognitive performance at the assessment closest to death.

Assessment of Other Clinical Covariates

We computed age at the time of cognitive assessment form the self-reported date of birth and date of assessment. We computed age at death from the self-reported date of birth and the date of death. We recorded sex at the time of the baseline interview. History of smoking (any vs. none) and alcohol consumption (converted to grams per day) were assessed at the time of the baseline interview.

Other Neuropathological Evaluation

Alzheimer's disease pathology was quantified as described previously (*42*). Neurofibrillary tangles, diffuse plaques, and neuritic plaques were visualized by Bielschowsky silver staining in sections from the frontal, temporal, parietal, and entorhinal cortices and the hippocampus. To generate a composite continuous measure of the burden of Alzheimer's disease pathology, neurofibrillary tangles, diffuse plaques, and neuritic plaques were counted in the regions above, the raw counts were divided by the standard deviation of the same index for that region across the entire cohort, and the scaled scores were averaged as described previously (*42*).

To quantify Lewy body pathology, 6 micron paraffin-embedded sections from the cingulate, entorhinal, midfrontal, middle temporal, and inferior parietal cortices and the substantia nigra were immunostained with antibodies to alpha synuclein (pSyn-64; 1:20,000; Wako Chemical USA Inc; Richmond, VA). Lewy body pathology was considered to be present if seen in any of these areas.

Macroscopic cerebral infarcts were identified by visual inspection of 1cm coronal slabs, and confirmed by histological review as previously described (*47*). Microscopic infarcts were quantified in a minimum of 9 regions (6 cortical and 3 subcortical) as previously described (*48*).

TDP-43 immunohistochemistry was performed on sections from 6 brain regions as previously described (*49*) using a rat phosphyorylated monoclonal TAR5P-1D3 (pS409410; 1:100; Aswcenion, Munich, Germany) TDP-43 antibody. Our primary measure was the presence of any extra-limbic TDP-43 pathology.

Hippocampal sclerosis was evaluated unilaterally in a coronal section of the mid-hippocampus at the level of the lateral geniculate body, and graded as absent or present based on severe neuronal loss and gliosis in CA1 and/or subiculum (*50*).

Assessment of Dorsolateral Prefrontal Gene Expression

RNA sequencing was performed on blocks of dorsolateral prefrontal cortex from a subset of ROS and MAP participants as previously described (*51, 52*). Nanodrop (Thermo Fisher Scientific, Waltham, MA) was used to quantify RNA extracted from dorsolateral prefrontal cortex blocks. Quality was analyzed using an Agilent Bioanalyzer. We excluded samples from which less than 5ug of RNA were obtained, or samples with a RNA integrity (RIN) score of 5 or less, from further analysis. The strand-specific dUTP method (*53*) with poly-A selection (*54*) was used by the Broad Institute Genomics Platform to prepare the RNA sequencing library. Poly-A selection was followed by first strand specific cDNA synthesis, with dUTP used for second strand specific cDNA synthesis, followed by fragmentation and Illumina adapter ligation for library construction. An Illumina HiSeq machine was used to perform sequencing with 101 bp paired-end reads, achieving a coverage of 150M reads for the first 12 samples, and 50M reads for the remaining samples. Beginning and ending low quality bases and adapter sequences were trimmed from the reads, and ribosomal RNA reads were removed. Bowtie 1 software (*55*) was used to align the reads to the reference genome. RSEM software was used to estimate, in units of fragments per kilobase per million mapped fragments (FPKM), expression levels for 55,889 individual GENCODE v14 genes, which were then quantile-normalized, correcting for batch effect with Combat (*56*). All FPKM values were log-transformed prior to further analysis. These data are available through the synapse.org AMP-AD Knowledge Portal (www.synapse.org SynapseID syn3388564). We analyzed only genes on autosomal chromosomes. Principal component analysis was used to assess sample quality, and only those samples with principal components 1, 2, and 3 values within 3 standard deviations from their respective means were included. Data from 622 ROS and MAP samples met all of the above these quality control criteria and were included in these analyses.

Supplemental Figures

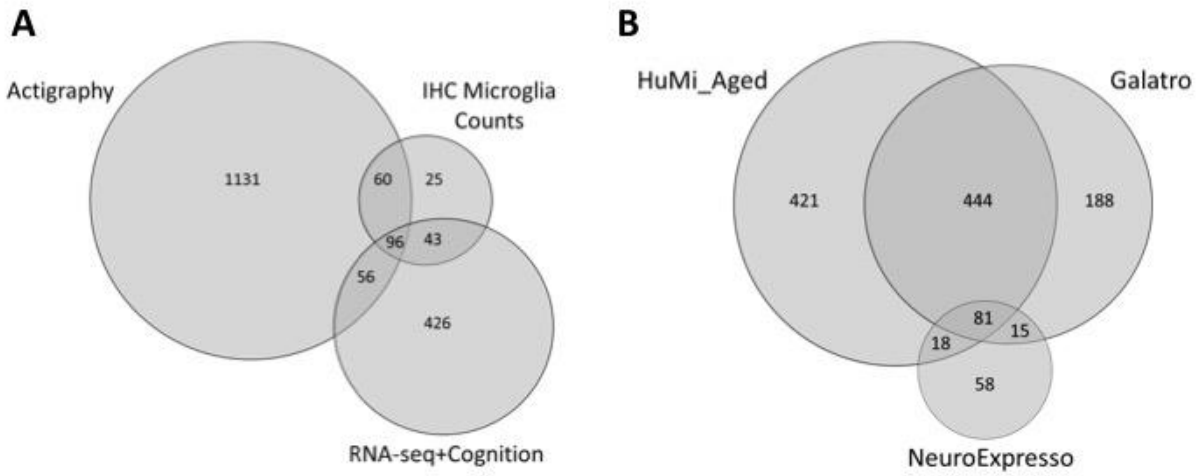

Fig. S1. Analytic subsets and microglial gene sets. (**A**) Intersection of Analytic Subsets. There were 622 participants with RNA-seq and cognitive evaluation of which 152 also had at least 1 actigraphic recording before death. There were 156 participants with immunohistochemical assessment of cortical microglial density and at least 1 actigraphic recording before death, of which 96 also had RNA-sequencing. (**B**) Intersection of Microglial Gene Sets. A total of 1225 genes from three microglial gene sets (HuMi_Aged; Galatro, and NeuroExpresso) were studied. There was substantial overlap between the two gene sets derived from human tissue with 72% of all genes in the Galatro gene set being also represented in the HuMi_Aged gene set. Similarly, 66% of the genes in the rodent-derived NeuroExpresso gene set are represented in at least 1 of the human microglial gene sets.

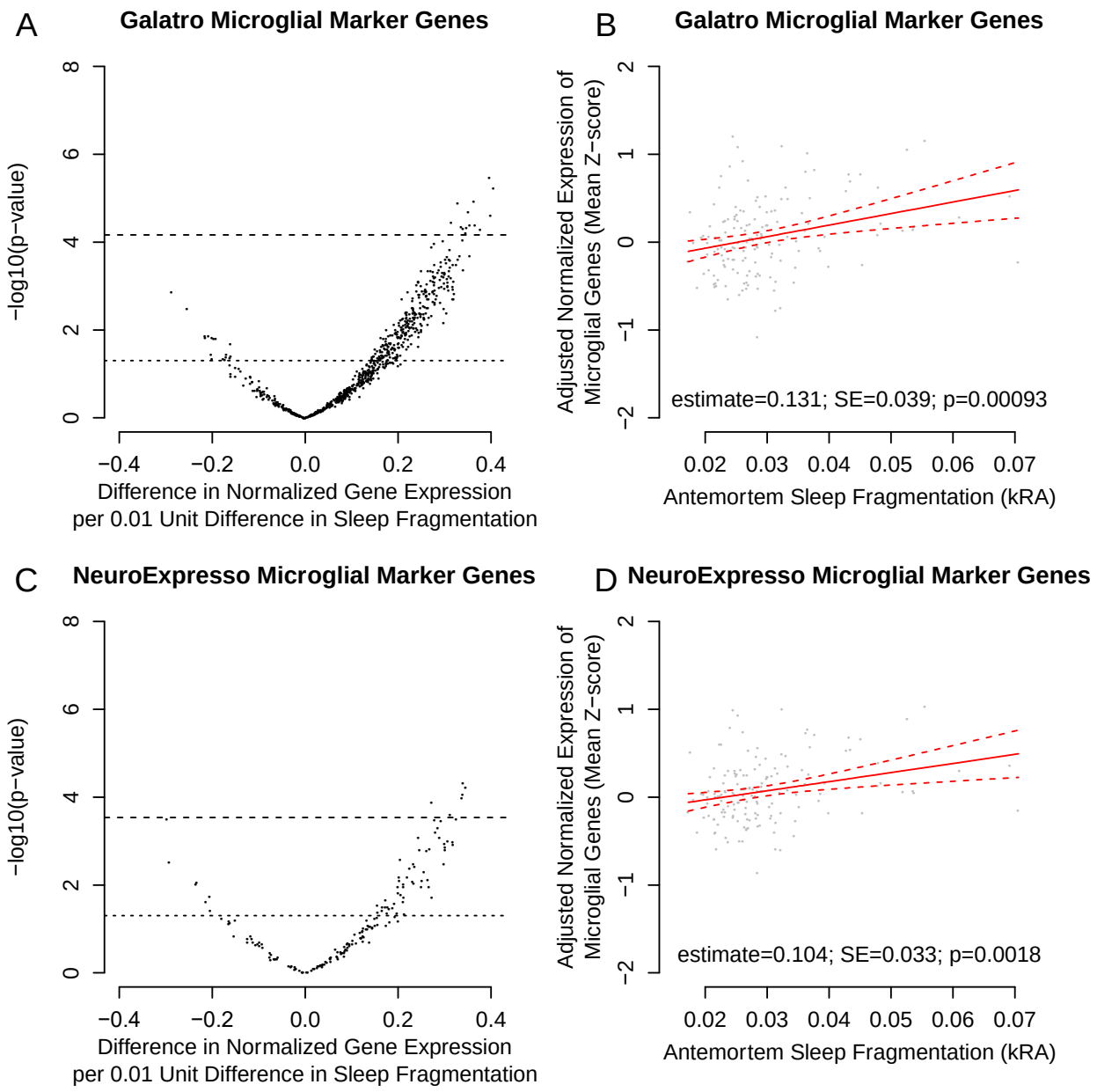

Fig. S2. Antemortem sleep fragmentation and expression of microglia marker genes in Galatro and NeuroExpresso microglial gene sets. (**A**-**B**) Galatro gene set. (**C**-**D**) NeuroExpresso gene set. (A, C) Volcano plots of –log10(p-value) vs. effect size for normalized gene expression as a function of antemortem sleep fragmentation, controlling for age at death, sex, education, and methodological covariates. Each dot represents a single gene. Dotted line 1qindicates unadjusted p<0.05. Dashed line indicates Bonferroni corrected p<0.05. (B, D) Partial residual plot of microglial gene expression summary score as a function of antemortem sleep fragmentation adjusted for age, sex, education, and methodological covariates. Y-axis is the composite expression for the gene set calculated as described in the text. X-axis is average antemortem sleep fragmentation. Each dot represents a single participant. Solid line indicates the predicted composite gene expression for an average participant. Dotted lines indicate 95% confidence intervals on the prediction.

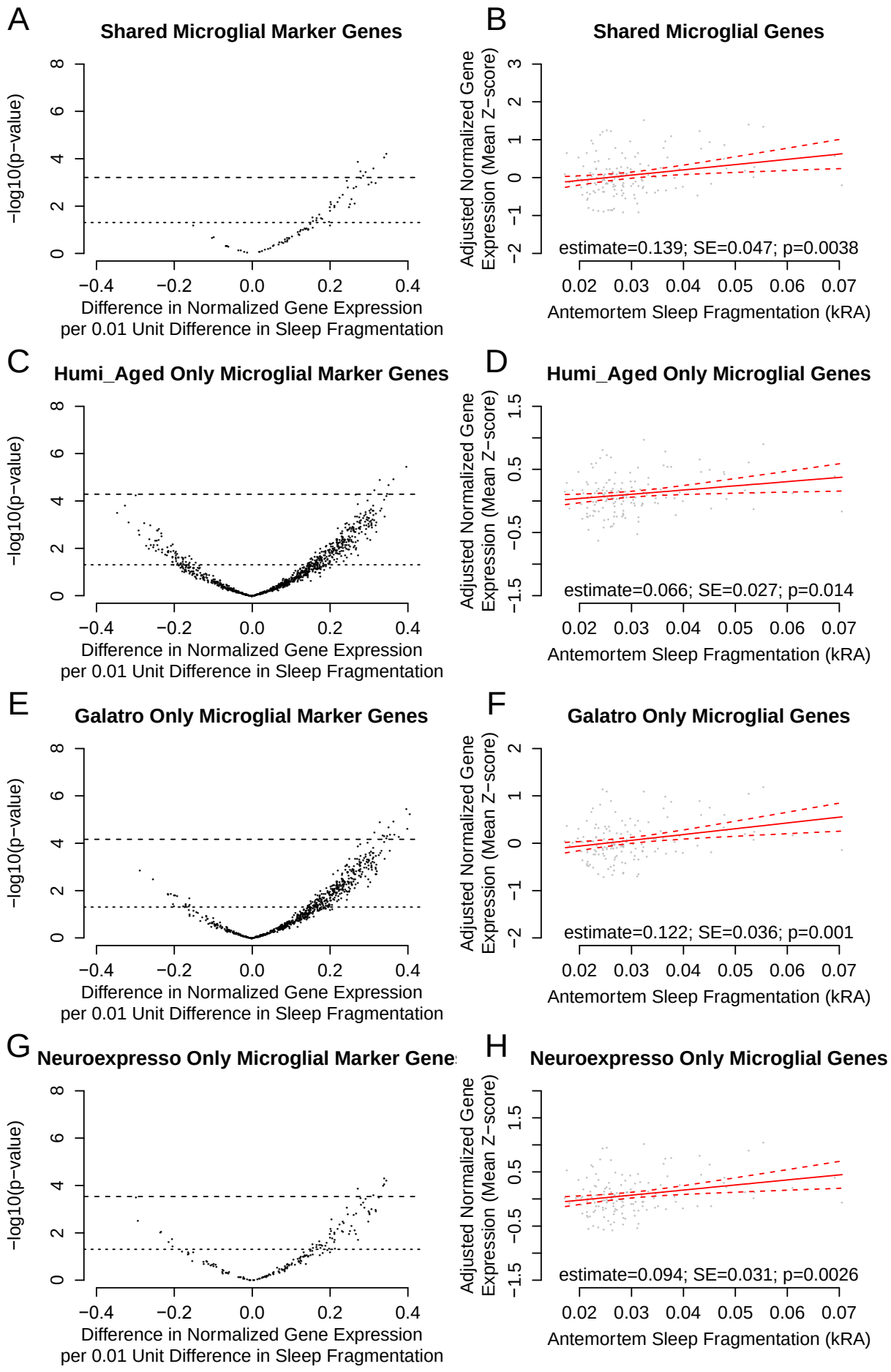
A
Shared Microglial Marker Genes
−log10(p−value)
Difference in Normalized Gene Expression
per 0.01 Unit Difference in Sleep Fragmentation
B
Shared Microglial Genes
Adjusted Normalized Gene Expression (Mean Z−score)
estimate=0.139; SE=0.047; p=0.0038
Antemortem Sleep Fragmentation (kRA)
C
Humi_Aged Only Microglial Marker Genes
D
Humi_Aged Only Microglial Genes
estimate=0.066; SE=0.027; p=0.014
E
Galatro Only Microglial Marker Genes
F
Galatro Only Microglial Genes
estimate=0.122; SE=0.036; p=0.001
G
Neuroexpresso Only Microglial Marker Gene
H
Neuroexpresso Only Microglial Genes
estimate=0.094; SE=0.031; p=0.0026

Fig. S3. Antemortem sleep fragmentation and expression of shared and unshared microglial marker genes from the HuMi_Aged, Galatro, and NeuroExpresso microglial gene sets. (A-B) Common genes (81 genes). (C-D) HuMi_Aged gene set unshared genes (421genes). (E-F) Galatro gene set unshared genes (188 genes). (G-H) NeuroExpresso gene set unshared genes (58 genes). (A, C, E, G): Volcano plots of –log10(p-value) vs. effect size for normalized gene expression as a function of antemortem sleep fragmentation, controlling for age at death, sex, education, and methodological covariates. Each dot represents a single gene. Dotted line indicates unadjusted $p<0.05$. Dashed line indicates Bonferroni corrected $p<0.05$. (B, D, F, H): Partial residual plot of microglial gene expression summary score as a function of antemortem sleep fragmentation adjusted for age, sex, education, and methodological covariates. Y-axis is the composite expression for the gene set calculated as described in the text. X-axis is average antemortem sleep fragmentation. Each dot represents a single participant. Solid line indicates the predicted composite gene expression for an average participant. Dotted lines indicate 95% confidence intervals on the prediction.

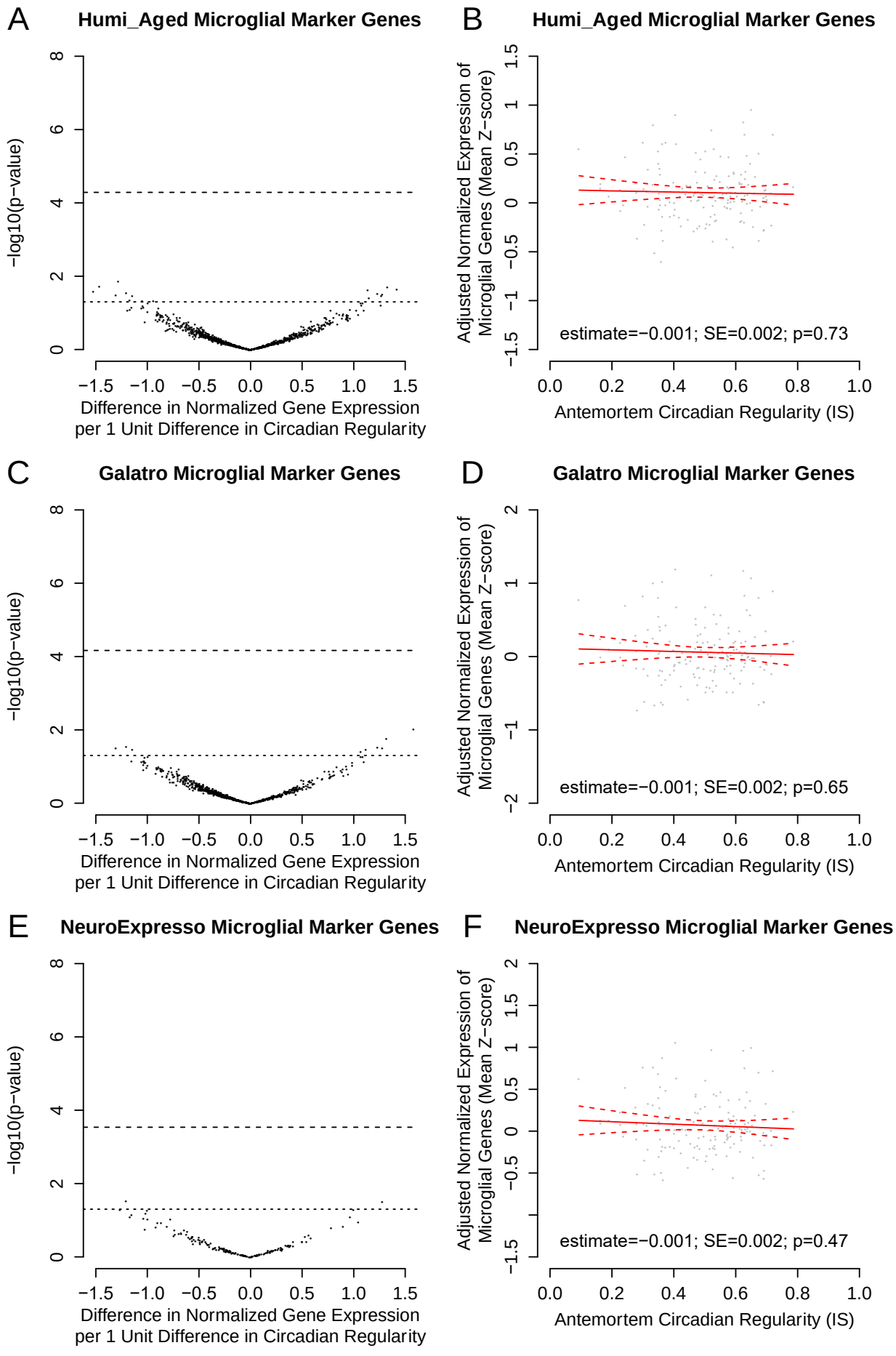
A
Humi_Aged Microglial Marker Genes
−log10(p−value)
Difference in Normalized Gene Expression
per 1 Unit Difference in Circadian Regularity
B
Humi_Aged Microglial Marker Genes
Adjusted Normalized Expression of
Microglial Genes (Mean Z−score)
estimate=−0.001; SE=0.002; p=0.73
Antemortem Circadian Regularity (IS)
C
Galatro Microglial Marker Genes
−log10(p−value)
Difference in Normalized Gene Expression
per 1 Unit Difference in Circadian Regularity
D
Galatro Microglial Marker Genes
Adjusted Normalized Expression of
Microglial Genes (Mean Z−score)
estimate=−0.001; SE=0.002; p=0.65
Antemortem Circadian Regularity (IS)
E
NeuroExpresso Microglial Marker Genes
−log10(p−value)
Difference in Normalized Gene Expression
per 1 Unit Difference in Circadian Regularity
F
NeuroExpresso Microglial Marker Genes
Adjusted Normalized Expression of
Microglial Genes (Mean Z−score)
estimate=−0.001; SE=0.002; p=0.47
Antemortem Circadian Regularity (IS)

Fig. S4. Antemortem circadian regularity and expression of microglial marker genes. (**A**-**B**) HuMi_Aged gene set. (**C**-**D**) Galatro gene set. (**E**-**F**) NeuroExpresso gene set. (A, C, E) Volcano plots of –log10(p-value) vs. effect size for normalized gene expression as a function of antemortem circadian regularity, controlling for age at death, sex, education, and methodological covariates. Each dot represents a single gene. Dotted line indicates unadjusted $p<0.05$. Dashed line indicates Bonferroni corrected $p<0.05$. (B, D, F) Partial residual plot of microglial gene expression summary score as a function of antemortem circadian regularity adjusted for age, sex, education, and methodological covariates. Y-axis is the composite expression for the gene set calculated as described in the text. X-axis is average antemortem circadian regularity. Each dot represents a single participant. Solid line indicates the predicted composite gene expression for an average participant. Dotted lines indicate 95% confidence intervals on the prediction.

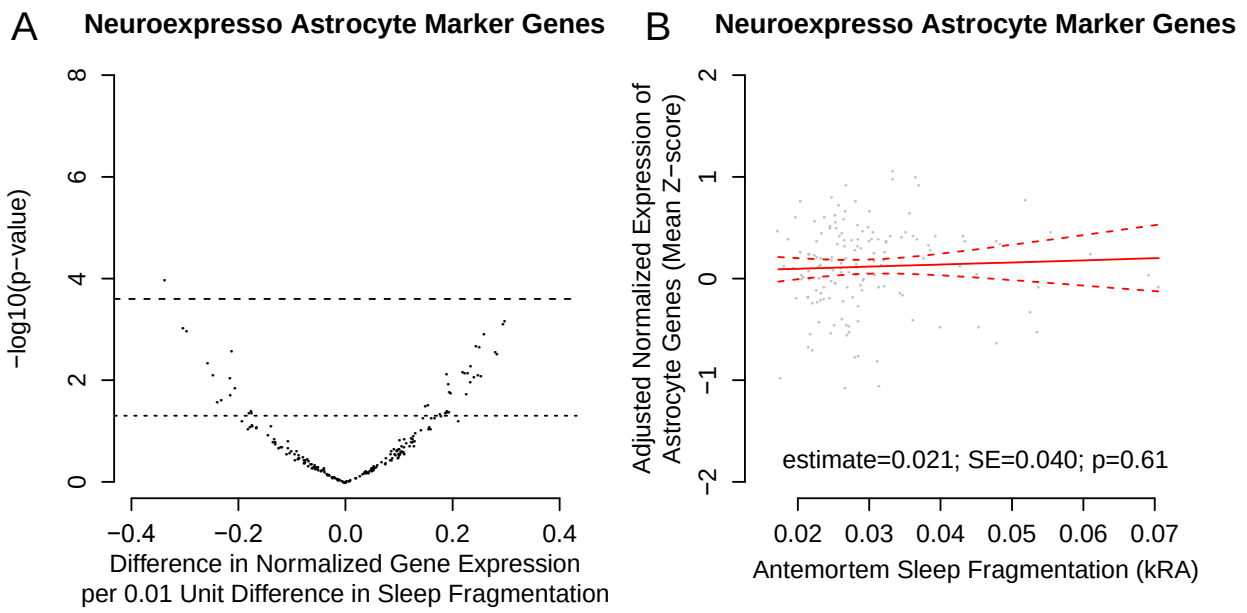

Fig. S5. Antemortem sleep fragmentation and expression of astrocytic marker genes. (**A**) Volcano plot of –log10(p-value) vs. effect size for normalized gene expression as a function of antemortem sleep fragmentation, controlling for age at death, sex, education, and methodological covariates. Each dot represents a single gene. Dotted line indicates unadjusted p<0.05. Dashed line indicates Bonferroni corrected p<0.05. (**B**) Partial residual plot of astrocytic gene expression summary score as a function of antemortem sleep fragmentation adjusted for age, sex, education, and methodological covariates. Y-axis is the composite expression for the gene set calculated as described in the text. X-axis is average antemortem sleep fragmentation. Each dot represents a single participant. Solid line indicates the predicted composite gene expression for an average participant. Dotted lines indicate 95% confidence intervals on the prediction.

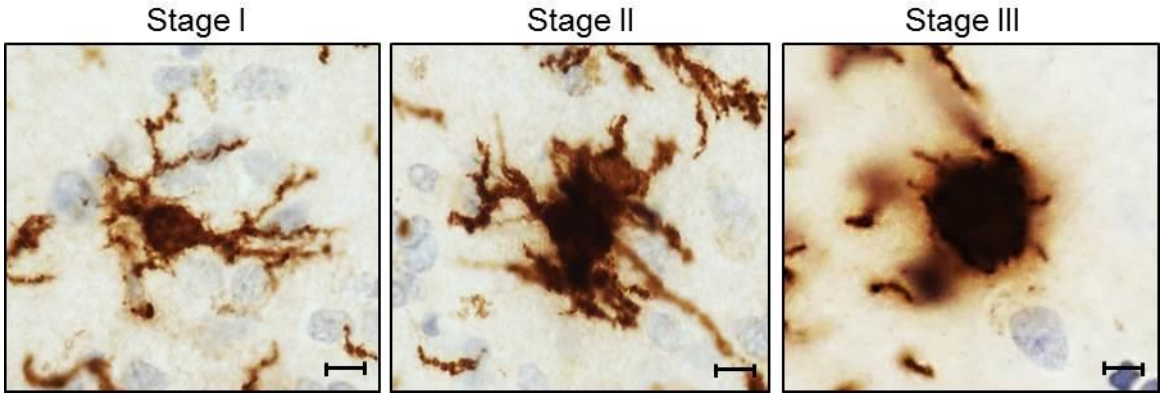

Fig. S6. Representative photomicrographs of microglial morphological stages. Scale bars are 10μm.

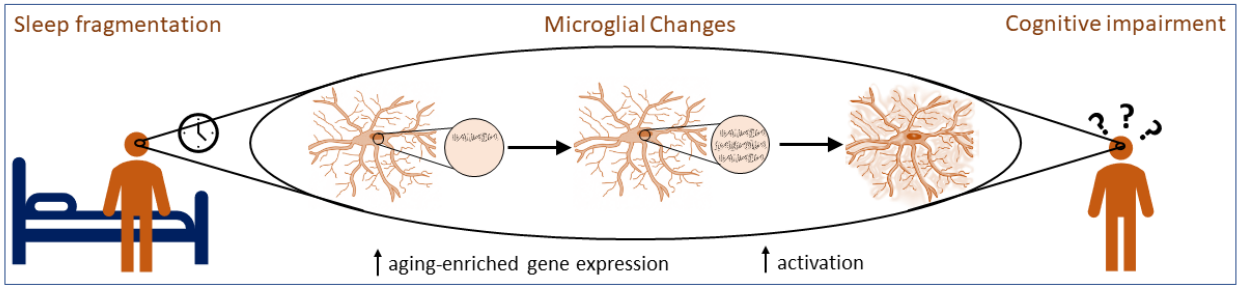

Fig. S7. Summary diagram. Sleep fragmentation is associated with changes in microglial biology, consisting of microglial aging which promotes microglial activation, which are in turn associated with cognitive impairment

Table S1. Antemortem sleep fragmentation and expression of microglia and astrocyte marker genes: Gene level results. Predictor = average antemortem sleep fragmentation. Outcome = gene expression normalized across all samples – only genes with non-zero expression in all samples. Models adjusted for age at death, sex, education, post-mortem interval, time between last assessment and death, RNA RIN score, and proportion of ribosomal bases. Effect estimate for difference in normalized gene expression per 0.01 unit change in sleep fragmentation. SE=standard error. P.val=p-value. Sheet 1: microglia marker genes from the HuMi_Aged, Galatro, and NeuroExpresso microglial gene sets meeting QC criteria and expressed at non-zero levels in all samples. Sheet 2: astrocyte marker genes from the NeuroExpresso astrocyte gene set.

See attached file Table_S1.csv

Table S2. Antemortem sleep fragmentation and composite expression of aging-enriched microglial genes: Adjustment for neuropathology. Predictor = average antemortem sleep fragmentation, normalized. Outcome = composite expression of HuMi-Aged genes characteristic of aged microglia. All models adjusted for age at death, sex, education, post-mortem interval, time between last assessment and death, RNA RIN score, and proportion of ribosomal bases.

Model	Outcome	Covariates	Predictor	Estimate	SE	Pval
A	Humi_Aged_Old	Age+Sex+Education+Technical*	Sleep	0.16	0.04	1.40E-04
B	Humi_Aged_Old	A+AD Pathology	Sleep	0.16	0.04	1.12E-04
C	Humi_Aged_Old	A+Lewy Body Pathology	Sleep	0.17	0.04	3.87E-05
D	Humi_Aged_Old	A+Gross Infarcts	Sleep	0.15	0.04	3.76E-04
E	Humi_Aged_Old	A+Micro Infarcts	Sleep	0.17	0.04	9.01E-05
F	Humi_Aged_Old	A+TDP43	Sleep	0.16	0.04	2.02E-04
G	Humi_Aged_Old	A+Hippocampal Sclerosis	Sleep	0.16	0.04	1.48E-04
H	Humi_Aged_Old	A+All Pathologies	Sleep	0.16	0.04	1.17E-04

*****post mortem interval, time between last assessment and death, RNA RIN score, proportion of ribosomal bases

Table S3. Antemortem sleep fragmentation, composite expression of genes characteristic of aged microglia, and proportion of activated microglia. All models adjusted for age at death, sex, education, post-mortem interval, time between last assessment and death, RNA RIN score, and proportion of ribosomal bases. Models A-D: Outcome is the composite expression of HuMi_Aged genes characteristic of aged microglia (HuMi_Aged_Old gene set). Predictors = sleep Fragmentation, density of microglia, or proportion of morphologically activated microglia, either alone (Models A, B, and C) or in combination (Model D). The association between sleep fragmentation and composite expression of HuMi_Aged_Old genes remains significant after controlling for density of microglia and proportion of morphologically activated microglia. Models E-G: Outcome is the proportion of stage II and III microglia. Model E: sleep fragmentation as predictor without microglial gene expression. Model F: composite expression of HuMi_Aged_Old genes as predictor, without sleep fragmentation. Model G: model including both sleep fragmentation and composite expression of HuMi_Aged_Old genes

		Predictor			
Model	Outcome	Sleep Fragmentation Estimate (SE) Pval	Density of Microglia Estimate (SE) Pval	% Activated Microglia Estimate (SE) Pval	Humi_Aged Old Gene Expression Estimate (SE) Pval
A	Humi_Aged_Old	0.14 (0.047) 0.0031			
B	Humi_Aged_Old		-0.012 (0.05) 0.81		
C	Humi_Aged_Old			0.078 (0.05) 0.13	
D	Humi_Aged_Old	0.13 (0.047) 0.0057	-0.028 (0.048) 0.56	0.064 (0.05) 0.2	
E	%Activated Microglia	0.04 (0.03) 0.19			
F	%Activated Microglia				0.05 (0.032) 0.13
G	%Activated Microglia	0.029 (0.032) 0.37			0.04 (0.034) 0.24

Table S4. Sleep fragmentation, expression of microglial genes, microglial activation, and composite global cognition proximate to death. Outcome for all models is composite global cognition proximate to death. All models adjusted for age ad death, sex, education, post-mortem interval, and time between last actigraphy and death. Models A-L additionally adjusted for RNA RIN score and proportion of ribosomal bases. Models A-H: Composite Expression of Genes Characteristic of Aged Microglia and Cognition Proximate to Death. All participants with RNA-seq (n=622); Predictor = composite expression of genes characteristic of aged microglia (HuMi_Aged_Old gene set). Models I-L: Sleep Fragmentation and Composite Global Cognition Proximate to Death – Effect of Adjusting for Neuropathology and Expression of Microglial Marker Genes. All participants with actigraphy and RNA-seq (n=152); Predictor = average antemortem sleep fragmentation, normalized. Model J adjusted for composite expression of genes characteristic of aged microglia (Humi_Aged_Old). Model K adjusted for burden of AD pathology, presence of Lewy Body pathology, presence of macroscopic infarcts, presence of microscopic infarcts, extra limbic TDP-43 pathology, and presence of hippocampal sclerosis. Model L adjusted for both microglial marker gene expression and brain pathologies. Models M-P: Sleep Fragmentation and Composite Global Cognition Proximate to Death – Effect of Adjusting for Neuropathology and Proportion of Activated Microglia. All participants with actigraphy and quantification of microglial density by immunohistochemistry (n=156). Predictor = average antemortem sleep fragmentation, normalized. Model N adjusted for proportion of morphologically activated microglia. Model O adjusted for burden of AD pathology, presence of Lewy Body pathology, presence of macroscopic infarcts, presence of microscopic infarcts, extra limbic TDP-43 pathology, and presence of hippocampal sclerosis. Model P adjusted for both proportion of morphologically activated microglia and brain pathologies.

Analytic Subgroup	Model	Outcome	Covariates	Predictor	Est	SE	Pval
Participants with RNA-seq (n=621)	A	Cognition	Age+Sex+Education+Technical+	Humi_Aged_Old	-0.13	0.05	9.49E-03
	B	Cognition	A+AD Pathology	Humi_Aged_Old	-0.10	0.04	2.10E-02
	C	Cognition	A+Lewy Body Pathology	Humi_Aged_Old	-0.13	0.05	1.09E-02
	D	Cognition	A+Gross Infarcts	Humi_Aged_Old	-0.14	0.05	4.92E-03
	E	Cognition	A+Micro Infarcts	Humi_Aged_Old	-0.13	0.05	7.46E-03
	F	Cognition	A+TDP43	Humi_Aged_Old	-0.11	0.05	3.36E-02
	G	Cognition	A+Hippocampal Sclerosis	Humi_Aged_Old	-0.12	0.05	1.41E-02
	H	Cognition	A+All Pathologies	Humi_Aged_Old	-0.1	0.05	3.75E-02
Actigraphy + RNA-seq (n-=152)	I	Cognition	Age+Sex+Education+Technical+	Sleep	-0.22	0.09	1.44E-02
	J	Cognition	I+Humi_Aged_Old	Sleep	-0.20	0.09	3.57E-02
	K	Cognition	I+All Pathologies	Sleep	-0.17	0.08	3.15E-02
	L	Cognition	K+Humi_Aged_Old	Sleep	-0.14	0.08	8.00E-02
Actigraphy + microglial density (n=156)	M	Cognition	Age+Sex+Education+Technical*	Sleep	-0.23	0.08	4.52E-03
	N	Cognition	M+% Activated Microglia	Sleep	-0.18	0.08	2.16E-02
	O	Cognition	M+All Pathologies	Sleep	-0.17	0.07	2.52E-02
	P	Cognition	O+% Activated Microglia	Sleep	-0.15	0.07	5.06E-02

+post mortem interval, time between last assessment and death, RNA RIN score, proportion of ribosomal bases

* postmortem interval and time between last assessment and death